ACS Macro Letters

pubs.acs.org/macroletters Letter

Excitation Dependence in Photoiniferter Polymerization

Rhys W. Hughes, Megan E. Lott, Jared I. Bowman, and Brent S. Sumerlin*

Cite This: ACS Macro Lett. 2023, 12, 14–19 Read Online

ACCESS | Metrics & More | Article Recommendations | Supporting Information

ABSTRACT: We report on a fundamental feature of photoiniferter polymerizations mediated with trithiocarbonates and xanthates. The polymerizations were found to be highly dependent on the activated electronic excitation of the iniferter. Enhanced rates of polymerization and greater control over molecular weights were observed for trithiocarbonate- and xanthate-mediated photoiniferter polymerizations when the n → π* transition of the iniferter was targeted compared to the polymerizations activating the π → π* transition. The disparities in rates of polymerization were attributed to the increased rate of C−S photolysis which was confirmed using model trapping studies. This study provides valuable insight into the role of electronic excitations in photoiniferter polymerization and provides guidance when selecting irradiation conditions for applications where light sensitivity is important.

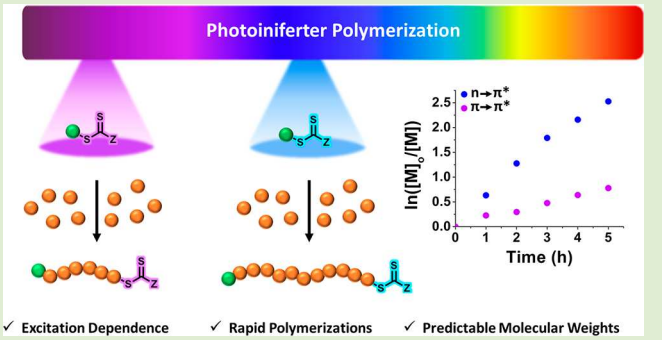

Many polymerization methods utilize heat as a stimulus to enable polymer synthesis, and reversible-deactivation radical polymerizations (RDRP) are no exception.[1,2] Reversible addition−fragmentation chain transfer (RAFT) polymerization offers controlled and tunable molecular weights as well as good functional group tolerance, allowing for the capability of polymerizing a wide array of monomers under relatively nonstringent conditions.[3−5] RAFT polymerization proceeds via radical generation by an exogenous radical initiator, usually driven by heat, in the presence of a thiocarbonylthio chain transfer agent that allows for the uniform growth of polymer chains by a degenerative chain transfer process.

The attractive nature of harnessing light to facilitate chemical synthesis has resulted in an increased exploration into photochemical reactions.[6] In particular, the spatiotemporal control offered by light is appealing in contrast to more conventional reactions initiated by heat.[7,8] As of late, there has been an increasing drive to expand the scope of RDRP techniques to afford well-controlled polymers under light-mediated conditions. Photoinduced atom transfer radical polymerization (ATRP) has emerged as a promising technique to achieve polymers with predictable molecular weights and low dispersities over a variety of radically polymerizable monomers (as well as bio-derived monomers) with low ppm catalyst loadings.[9−13] Photoinduced electron/energy transfer RAFT (PET-RAFT) polymerization employs a photoredox catalyst capable of transferring an electron/energy to a RAFT chain transfer agent, allowing for a controlled radical polymerization in the absence of conventional thermal initiators.[14−18] Surging interest in PET-RAFT polymerization has resulted in the resurfacing of chemistry first reported by Otsu, namely iniferter polymerization.[19] The light-mediated version of this chemistry (i.e., photoiniferter polymerization) utilizes the energy harnessed from light and employs a thiocarbonylthio molecule capable of initiation, chain transfer, and reversible termination (iniferter) to facilitate a well-controlled polymerization. The control afforded during a photoiniferter process relies on both degenerative chain transfer and reversible termination (Figure 1) to effect the activation−deactivation equilibrium which is the hallmark of all RDRP processes. While both RAFT and photoiniferter

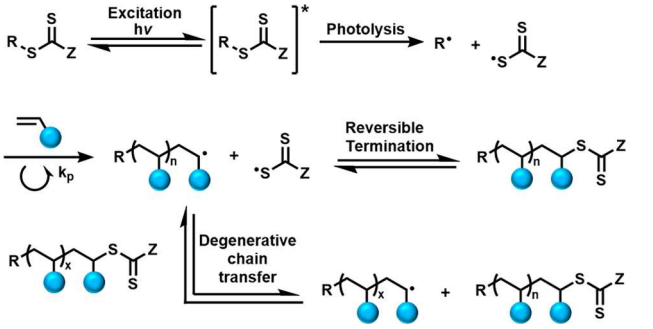

Figure 1. Proposed photoiniferter polymerization mechanism.

Received: November 21, 2022
Accepted: December 13, 2022
Published: December 19, 2022

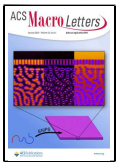

https://doi.org/10.1021/acsmacrolett.2c00683
ACS Macro Lett. 2023, 12, 14−19

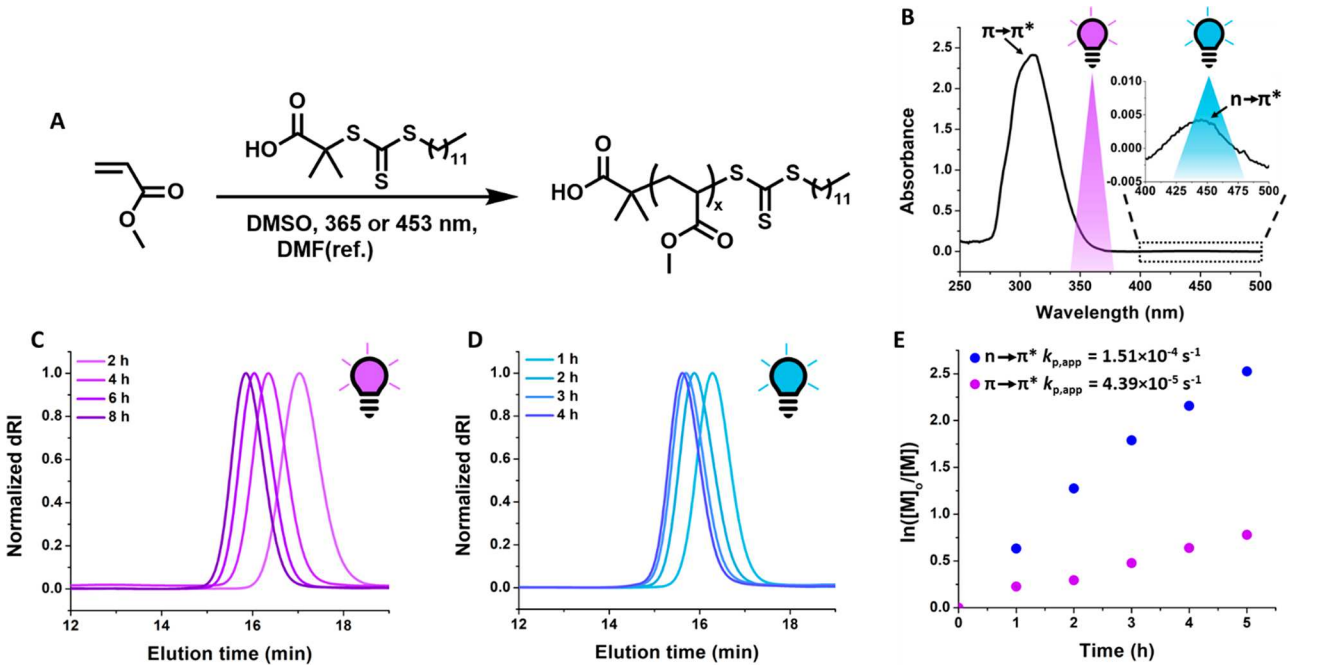

Figure 2. (A) Scheme for the photoiniferter polymerization of methyl acrylate (MA) with 2-(dodecylthiocarbonothioylthio)-2-methylpropionic acid (DDMAT) under different wavelengths of light. (B) UV−vis spectrum of DDMAT in dimethyl sulfoxide annotated with the location of the electronic excitations and the overlap of the absorbance with the wavelengths of light used as can be seen by the shaded regions. (C) Gel permeation chromatography (GPC) elugrams for the photoiniferter polymerization under 365 nm light. (D) GPC elugrams for the photoiniferter polymerization under 453 nm light. (E) Linear pseudo-first-order kinetic plot of the two trithiocarbonate-mediated photoiniferter polymerizations of MA under different wavelengths of light.

polymerizations typically rely on thiocarbonylthio compounds, the latter approach is notable because of the absence of an external initiator, instead relying on C−S bond photolysis to generate the radicals needed for propagation. The absence of exogenous initiator and the low molecular weight tailing that sometimes results make photoiniferter polymerizations particularly useful for a wide variety of applications, including for the synthesis of ultrahigh molecular weight polymers.[20−23] Photoiniferter polymerization not only has demonstrated the ability to afford well-controlled polymerizations under mild irradiation conditions and open to air but also has been used with orthogonal polymerization pathways, displaying the highly versatile nature of this approach.[23−27]

In the photoiniferter process, light excites an electron in the C═S bond of the iniferter into a higher energy state. The excited electron then either proceeds back to the ground state or results in C−S homolytic bond cleavage by β-scission. Photolysis of the C−S bond generates a carbon-centered radical capable of initiating polymerization and a less reactive thiocarbonylthiyl radical that can reversibly terminate growing polymer chains (Figure 1).[28,29]

The most commonly used photoiniferters are trithiocarbonates and xanthates.[30] Trithiocarbonates offer good control over monomers such as methacrylates, acrylates, and acrylamides, while xanthates offer good control over monomers such as vinyl esters and acrylamides.[31] Both trithiocarbonates and xanthates facilitate photoiniferter polymerization across the ultraviolet (UV) and visible regions of the light spectrum.[32−34] The rate and control of polymerization can be tuned by regulating the number of radicals generated by C−S photolysis, by tuning the wavelength or intensity of light, or by the stability of the carbon-centered radical formed upon photolysis.[35−39]

The targeted electronic excitations that can effect C−S homolysis in the UV and visible light range for iniferters are the $\pi \rightarrow \pi^*$ and the n $\rightarrow \pi^*$ electronic transitions. The energy gap for the n $\rightarrow \pi^*$ transition is smaller than that of the $\pi \rightarrow \pi^*$ transition. Consequently, the n $\rightarrow \pi^*$ transition is observed at longer wavelengths, while the $\pi \rightarrow \pi^*$ excitation is present at higher energy within the UV region.[32,40] On a valence electron examination, the $\pi \rightarrow \pi^*$ ($S_0 \rightarrow S_2$) involves the excitation of an electron from the C═S π orbital into the analogous antibonding orbital, whereas the n $\rightarrow \pi^*$ ($S_0 \rightarrow S_1 \rightarrow T_1$) involves the excitation of an electron from one of the lone pair electrons on the thiocarbonyl sulfur atom into the π^* antibonding orbital.[41] Due to the change in spin associated with the n $\rightarrow \pi^*$ transition, this forbids the spin selection rule and results in a much smaller extinction coefficient than for the $\pi \rightarrow \pi^*$ transition.[42]

As mentioned previously, photoiniferter polymerization has been conducted and compared at various wavelengths of light; however, few reports have offered insight into the potential differences in photoiniferter polymerization as a result of targeting specific electronic transitions. Moreover, most previous reports employing different wavelengths of irradiation have involved light sources with varying intensities, making direct comparisons somewhat difficult to interpret.[38,43,44] Due to the ubiquity of trithiocarbonates and xanthates used in photoiniferter polymerization, we sought to investigate the implications of targeting distinct electronic excitations on the rate and control during photoiniferter polymerization.

Our initial investigations began with 2-(dodecylthiocarbonothioylthio)-2-methylpropionic acid (DDMAT) as the iniferter for polymerization of methyl acrylate (MA) in dimethyl sulfoxide (DMSO) (Figure 2A). The $\pi \rightarrow \pi^*$ transition for DDMAT occurs at 310 nm, while the n $\rightarrow \pi^*$ occurs at 445

https://doi.org/10.1021/acsmacrolett.2c00683
ACS Macro Lett. 2023, 12, 14−19

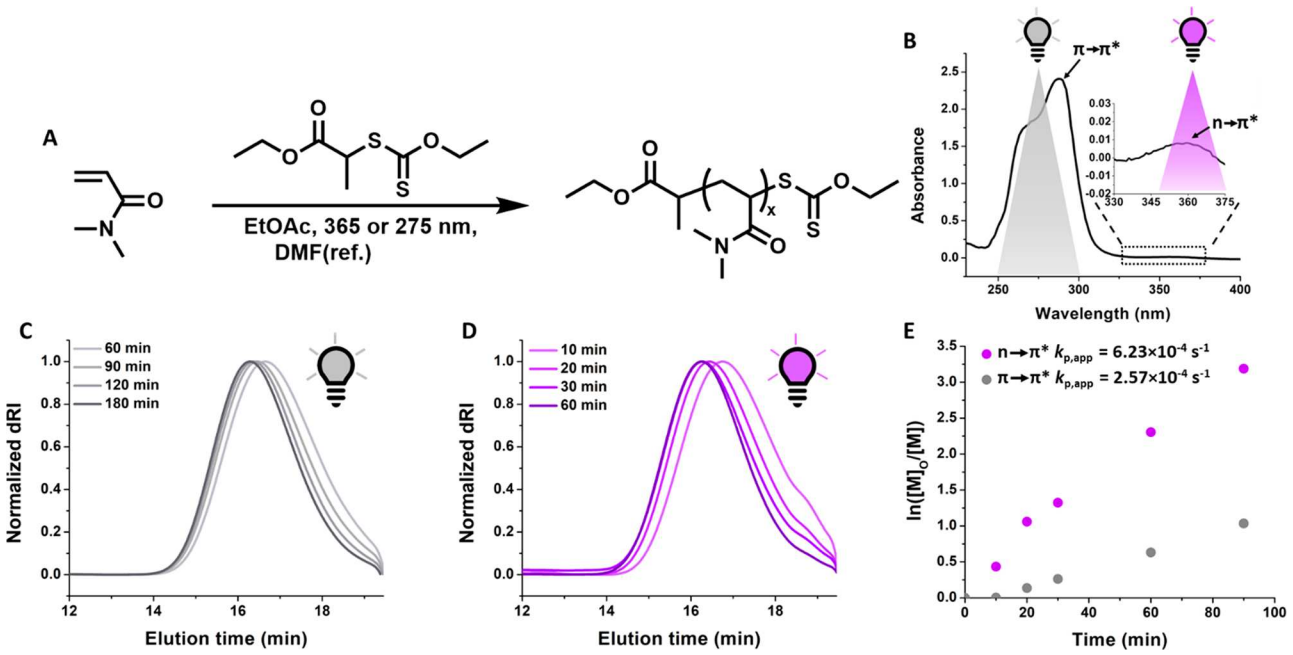

Figure 3. (A) Polymerization scheme of *N*,*N*-dimethylacrylamide (DMA) with 2-(ethoxycarbonothioyl)sulfanyl propanoate (EXEP). (B) UV−vis spectrum of EXEP in ethyl acetate annotated with the location of the electronic excitations and the overlap of the absorbance with the wavelengths of light as can be seen by the shaded regions. (C) Gel permeation chromatography (GPC) elugrams for the photoiniferter polymerization of DMA under 275 nm light. (D) GPC elugrams for the photoiniferter polymerization of DMA under 365 nm light. (E) Linear pseudo-first-order kinetic plot of the two xanthate-mediated photoiniferter polymerizations of DMA under different wavelengths of light.

nm (Figure 2B). To access these transitions, light-emitting diodes (LEDs) of either 365 nm (UV) or 453 nm (blue) were used with identical and constant intensities of 0.6 mW/cm^2. Despite poorer overlap of the $\pi \rightarrow \pi^*$ transition with the 365 nm light source, the extinction coefficient at this wavelength is much greater than that of the n $\rightarrow \pi^*$ transition (ε = 151 M^{-1} cm^{-1} at 365 nm, ε = 35.4 M^{-1} cm^{-1} at 453 nm). Photoiniferter polymerizations performed at both wavelengths resulted in well-controlled, unimodal polymers with low dispersities and number-average molecular weights in close agreement with theoretical values (Figure 2C, D). However, substantial differences in the rates of polymerization were observed (Figure 2E). The polymerization under blue light, accessing the n $\rightarrow \pi^*$ excitation, afforded a polymerization with 96% conversion after 8 h, while the corresponding polymerization under UV light required 21 h to reach a similar conversion (Table S1, entries 1, 2)). The apparent rate constant of propagation ($k_{p,app}$) for the polymerization under blue light was 1.51 × 10^{-4} s^{-1}, while the polymerization under UV light was more than 3 times slower, with a $k_{p,app}$ of 4.39 × 10^{-5} s^{-1}.

This difference in rate as a function of irradiation wavelength was also observed during the polymerization of an acrylamido monomer (*N*,*N*-dimethylacrylamide (DMA)) mediated with another trithiocarbonate (Figure S10), namely 2-(((ethylthio)-carbonothioyl)thio)propanoic acid (PAETC) (Table S1, entries 3, 4). Targeting the n $\rightarrow \pi^*$ transitions of the trithiocarbonates resulted in polymers that agreed slightly better with theoretical molecular weights, which may be due to the prolonged exposure required for the trithiocarbonate end-group during irradiation with UV light when accessing the $\pi \rightarrow \pi^*$ transition.[36,45] We believe the increased rate and control offered by using lower energy light to target the n $\rightarrow \pi^*$ transition are consistent with a general trend for trithiocarbonate-mediated photoiniferter polymerizations.

To further explore the dependence of the targeted electronic transition of the iniferter on the polymerization rate and molecular weight control, we extended our studies to xanthate-mediated photoiniferter polymerizations. The UV−vis spectrum of 2-(ethoxycarbonothioyl)sulfanyl propanoate (EXEP) (Figure 3B) shows a strong absorption for the $\pi \rightarrow \pi^*$ transition at 287 nm and a much weaker absorption for the n $\rightarrow \pi^*$ transition at 357 nm. To target these transitions, 275 and 365 nm LEDs with identical and constant light intensities of 0.1 mW/cm^2 were used to conduct the polymerization of DMA (Figure 3A). As expected, the xanthate provided slightly less molecular weight control than the trithiocarbonate photoiniferter, resulting in poly(DMA) (PDMA) with dispersities of 1.39−1.45 in 3 h or less (Table S1, entries 5, 6). We again observed that excitation of the n $\rightarrow \pi^*$ transition led to a much faster rate of polymerization than when targeting the $\pi \rightarrow \pi^*$ transition (Figure 3E), as quantified by the $k_{p,app}$ for the n $\rightarrow \pi^*$ and $\pi \rightarrow \pi^*$ transitions being 6.23 × 10^{-4} s^{-1} and 2.57 × 10^{-4} s^{-1}, respectively. Photoiniferter polymerizations using EXEP also afforded polymers of MA (Table S1, entries 7, 8) and methyl methacrylate (MMA). Interestingly, while xanthates are poor polymerization mediators for methacrylates, slightly better molecular weight control was observed for the polymerization of MMA when activating the n $\rightarrow \pi^*$ transition (Table S1, entries 9, 10). To expand the scope of xanthates, a more hydrophilic xanthate was also used, namely 2-((ethoxycarbonothioyl)thio)propionic acid (EXAP), for the photoiniferter polymerization of DMA to demonstrate the ability to transfer these polymerizations to aqueous systems. The observed differences in rate of polymerization as a function of the excited electronic transition of the iniferter was also present in this system, leading us to propose that this is a general trend for xanthate-mediated photoiniferter polymerizations (Figure S13).

https://doi.org/10.1021/acsmacrolett.2c00683
ACS Macro Lett. 2023, 12, 14−19

To confirm that the disparity in rates for the xanthate-mediated photoiniferter polymerizations was not due to decreased light penetration at 275 nm as a result of the glass reaction vessel, model polymerizations were also performed in quartz cuvettes. Indeed, polymerizations with light sources targeting the n → π* transition again proceeded with higher rates compared to those targeting the π → π* transition (Table S1, entries 13, 14).

The rapid rates of polymerization of xanthates in comparison to trithiocarbonates can be explained by the faster C−S photolysis of xanthates due to the difference in bond dissociation energies. By density functional theory calculations, the C−S bond in xanthates has been calculated to be ∼3.4 kcal/mol weaker than in trithiocarbonates.[46] As mentioned previously, regardless of the polymerization conditions employed, higher dispersities were observed for the xanthate-mediated polymerizations relative to the trithiocarbonate-mediated polymerizations. We attribute this to the lower chain transfer constants of xanthates leading to a reduced rate of exchange via degenerative transfer.[47] The disparity in rates of polymerization when accessing the different electronic transitions for both trithiocarbonates and xanthates is most likely explained by the higher quantum yield associated with the n → π* transition, meaning that accessing this transition yields more rapid C−S photolysis and a concomitant increase in radical concentration.

To test the hypothesis that the increased rate of polymerization can be attributed to accelerated photolysis when targeting the n → π* transition, model trapping studies were undertaken. Low molecular weight PDMA polymers terminated with either trithiocarbonate (PDMA-TTC) or xanthate (PDMA-Xan) moieties were irradiated in the presence of 2,2,6,6-tetramethylpiperidine-1-oxyl (TEMPO) as a model radical trapping agent (Figure 4A). To investigate the rate of photolysis, we used ^{1}H NMR spectroscopy to monitor the disappearance of the methine proton on the ω-terminus of PDMA-TTC and PDMA-Xan as a function of irradiation time in the presence of TEMPO. Irradiating PDMA-TTC at 453 nm for 4 h resulted in the consumption of 58% of the trithiocarbonate, while only 32% was consumed during irradiation at 365 nm (Figure 4B). Similarly, irradiating PDMA-Xan at 365 nm for 90 min resulted in 87% loss of xanthate end-groups, while only 60% was lost over the same period with 275 nm light (Figure 4C). These results are consistent with the hypothesis that the differences in the rate of photoiniferter polymerization when targeting the n → π* transition of both trithiocarbonates and xanthates are due to an increased rate of C−S photolysis.

As mentioned previously for the trithiocarbonate-mediated polymerizations, activation of both the n → π* transition and the π → π* transition led to polymers in close agreement with theoretical molecular weights, although a slight increase in molecular weight control was achieved when the n → π* transition of the iniferter was targeted. Interestingly, activating the n → π* of the iniferter for the xanthate-mediated polymerizations mostly led to polymers with lower dispersities than those achieved by activating the π → π* transition. The increased molecular weight control is more evident for the polymerizations of MMA in which closer agreement with theoretical molecular weights was achieved by activating the n → π* transition. Because of the low chain transfer constant of xanthates during the polymerization of methacrylates, we attribute the enhanced molecular weight control to faster

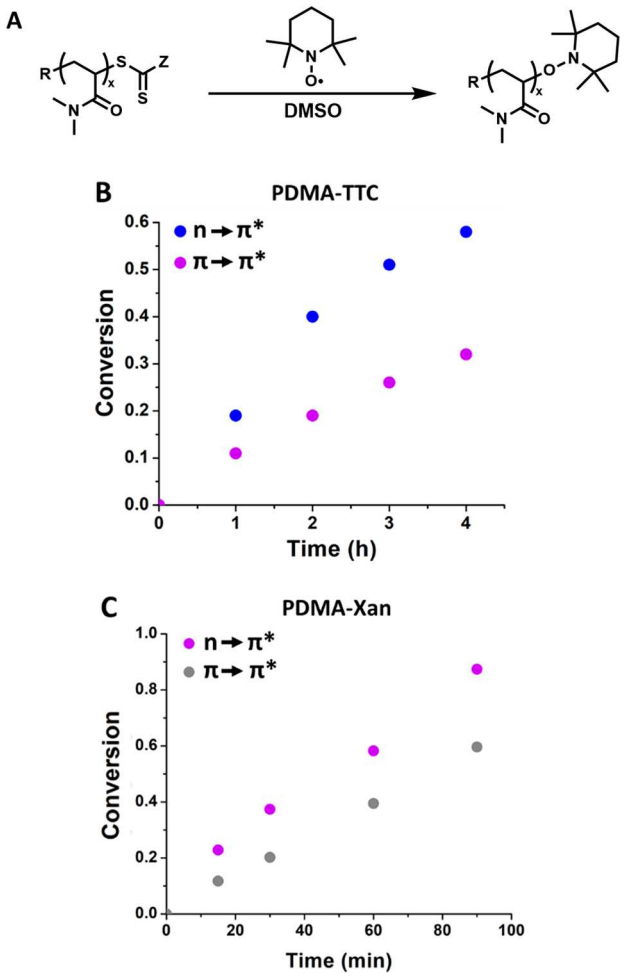

Figure 4. (A) 2,2,6,6-Tetramethylpiperidine-1-oxyl (TEMPO) trapping kinetics during irradiation of low molecular weight (B) poly(*N*,*N*-dimethylacrylamide)−trithiocarbonate (PDMA-TTC) and (C) poly(*N*,*N*-dimethylacrylamide)−xanthate (PDMA-Xan). These results offer insight into the relative photolysis kinetics when targeting specific electronic transitions.

photolysis that effectively equates to an increased rate of initiation which allows for the more uniform growth of chains.

In conclusion, we have elucidated the effects of different electronic excitations of various iniferters in photoiniferter polymerization. Perhaps counterintuitively, using lower energy light to access the n → π* transition allowed for more efficient activation of iniferters, despite the stronger absorption from the π → π* transition in the UV region. These results have important implications for selecting conditions during photoiniferter polymerizations and even for the photoinduced end-group removal of polymers bearing trithiocarbonate or xanthate chain ends. Moreover, by targeting specific electronic transitions of the end-group moiety in photoiniferter polymerization, it is possible to tune both the rate and extent of molecular weight control. Additionally, because accelerated polymerizations can be achieved by careful targeting of specific electronic transitions, lower light intensities can be employed, suggesting that photoiniferter polymerization may be more amenable for applications where light sensitivity is important.

https://doi.org/10.1021/acsmacrolett.2c00683
ACS Macro Lett. 2023, 12, 14−19

■ ASSOCIATED CONTENT

Supporting Information

The Supporting Information is available free of charge at https://pubs.acs.org/doi/10.1021/acsmacrolett.2c00683.

Materials, experimental procedures, analyses, and additional data (PDF)

■ AUTHOR INFORMATION

Corresponding Author

Brent S. Sumerlin − *George & Josephine Butler Polymer Research Laboratory, Center for Macromolecular Science & Engineering, Department of Chemistry, University of Florida, Gainesville, Florida 32611, United States;* orcid.org/0000-0001-5749-5444; Email: sumerlin@chem.ufl.edu

Authors

Rhys W. Hughes − *George & Josephine Butler Polymer Research Laboratory, Center for Macromolecular Science & Engineering, Department of Chemistry, University of Florida, Gainesville, Florida 32611, United States;* orcid.org/0000-0003-1751-051X

Megan E. Lott − *George & Josephine Butler Polymer Research Laboratory, Center for Macromolecular Science & Engineering, Department of Chemistry, University of Florida, Gainesville, Florida 32611, United States;* orcid.org/0000-0001-9854-6252

Jared I. Bowman − *George & Josephine Butler Polymer Research Laboratory, Center for Macromolecular Science & Engineering, Department of Chemistry, University of Florida, Gainesville, Florida 32611, United States;* orcid.org/0000-0001-6469-2251

Complete contact information is available at: https://pubs.acs.org/10.1021/acsmacrolett.2c00683

Author Contributions

CRediT: **Rhys William Hughes** conceptualization (equal), data curation (equal), formal analysis (equal), investigation (equal), methodology (equal), validation (equal), writing-original draft (equal), writing-review & editing (equal); **Megan E. Lott** conceptualization (equal), data curation (equal), formal analysis (equal), investigation (equal), methodology (equal), validation (equal), writing-review & editing (equal); **Jared I. Bowman** conceptualization (equal), data curation (equal), formal analysis (equal), investigation (equal), methodology (equal), validation (equal), writing-review & editing (equal); **Brent S. Sumerlin** conceptualization (equal), project administration (equal), resources (equal), software (equal), supervision (equal), visualization (equal), writing-review & editing (equal).

Funding

This material is based on work supported by the National Science Foundation (DMR-1904631) and DoD through the ARO (W911NF-17-1-0326).

Notes

The authors declare no competing financial interest.

■ REFERENCES

(1) Storey, R. F. Fundamental Aspects of Living Polymerization. In *Fundamentals of Controlled/Living Radical Polymerization*; Tsarevsky, N. V., Sumerlin, B. S., Eds.; The Royal Society of Chemistry: Cambridge, 2013; pp 60−77.

(2) Matyjaszewski, K. Fundamentals of Controlled/Living Radical Polymerization. In *Encyclopedia of Radicals in Chemistry, Biology and Materials*; John Wiley & Sons: 2012; pp 2−24.

(3) Hill, M. R.; Carmean, R. N.; Sumerlin, B. S. Expanding the Scope of RAFT Polymerization: Recent Advances and New Horizons. *Macromolecules* **2015**, *48*, 5459−5469.

(4) Garrison, J. B.; Hughes, R. W.; Young, J. B.; Sumerlin, B. S. Photoinduced SET to Access Olefin-Acrylate Copolymers. *Polym. Chem.* **2022**, *13*, 982−988.

(5) Garrison, J. B.; Hughes, R. W.; Sumerlin, B. S. Backbone Degradation of Polymethacrylates via Metal-Free Ambient-Temperature Photoinduced Single-Electron Transfer. *ACS Macro Lett.* **2022**, *11*, 441−446.

(6) Chen, M.; Zhong, M.; Johnson, J. A. Light-Controlled Radical Polymerization: Mechanisms, Methods, and Applications. *Chem. Rev.* **2016**, *116*, 10167−10211.

(7) Olson, R. A.; Korpusik, A. B.; Sumerlin, B. S. Enlightening Advances in Polymer Bioconjugate Chemistry: Light-Based Techniques for Grafting to and from Biomacromolecules. *Chem. Sci.* **2020**, *11*, 5142−5156.

(8) Chatani, S.; Kloxin, C. J.; Bowman, C. N. The Power of Light in Polymer Science: Photochemical Processes to Manipulate Polymer Formation, Structure, and Properties. *Polym. Chem.* **2014**, *5*, 2187−2201.

(9) Konkolewicz, D.; Schröder, K.; Buback, J.; Bernhard, S.; Matyjaszewski, K. Visible Light and Sunlight Photoinduced ATRP with ppm of Cu Catalyst. *ACS Macro Lett.* **2012**, *1*, 1219−1223.

(10) Parkatzidis, K.; Boner, S.; Wang, H. S.; Anastasaki, A. Photoinduced Iron-Catalyzed ATRP of Renewable Monomers in Low-Toxicity Solvents: A Greener Approach. *ACS Macro Lett.* **2022**, *11*, 841−846.

(11) Dadashi-Silab, S.; Pan, X.; Matyjaszewski, K. Photoinduced Iron-Catalyzed Atom Transfer Radical Polymerization with ppm Levels of Iron Catalyst under Blue Light Irradiation. *Macromolecules* **2017**, *50*, 7967−7977.

(12) Pan, X.; Malhotra, N.; Simakova, A.; Wang, Z.; Konkolewicz, D.; Matyjaszewski, K. Photoinduced Atom Transfer Radical Polymerization with ppm-Level Cu Catalyst by Visible Light in Aqueous Media. *J. Am. Chem. Soc.* **2015**, *137*, 15430−15433.

(13) Szczepaniak, G.; Jeong, J.; Kapil, K.; Dadashi-Silab, S.; Yerneni, S. S.; Ratajczyk, P.; Lathwal, S.; Schild, D. J.; Das, S. R.; Matyjaszewski, K. Open-Air Green-Light-Driven ATRP Enabled by Dual Photoredox/Copper Catalysis. *Chem. Sci.* **2022**, *13*, 11540−11550.

(14) Figg, C. A.; Hickman, J. D.; Scheutz, G. M.; Shanmugam, S.; Carmean, R. N.; Tucker, B. S.; Boyer, C.; Sumerlin, B. S. Color-Coding Visible Light Polymerizations to Elucidate the Activation of Trithiocarbonates Using Eosin y. *Macromolecules* **2018**, *51*, 1370−1376.

(15) Allegrezza, M. L.; Konkolewicz, D. PET-RAFT Polymerization: Mechanistic Perspectives for Future Materials. *ACS Macro Lett.* **2021**, *10*, 433−446.

(16) Korpusik, A. B.; Tan, Y.; Garrison, J. B.; Tan, W.; Sumerlin, B. S. Aptamer-Conjugated Micelles for Targeted Photodynamic Therapy via Photoinitiated Polymerization-Induced Self-Assembly. *Macromolecules* **2021**, *54*, 7354−7363.

(17) Lessard, J. J.; Scheutz, G. M.; Korpusik, A. B.; Olson, R. A.; Figg, C. A.; Sumerlin, B. S. Self-Catalyzing Photoredox Polymerization for Recyclable Polymer Catalysts. *Polym. Chem.* **2021**, *12*, 2205−2209.

(18) Olson, R. A.; Levi, J. S.; Scheutz, G. M.; Lessard, J. J.; Figg, C. A.; Kamat, M. N.; Basso, K. B.; Sumerlin, B. S. Macromolecular Photocatalyst for Synthesis and Purification of Protein-Polymer Conjugates. *Macromolecules* **2021**, *54*, 4880−4888.

(19) Otsu, T.; Yoshida, M. Role of Initiator-Transfer Agent-Terminator (Iniferter) in Radical Polymerizations: Polymer Design by Organic Disulfides as Iniferters. *Makromol. Chem. Rapid Commun.* **1982**, *3*, 127−132.

(20) Carmean, R. N.; Sims, M. B.; Figg, C. A.; Hurst, P. J.; Patterson, J. P.; Sumerlin, B. S. Ultrahigh Molecular Weight Hydrophobic Acrylic and Styrenic Polymers through Organic-Phase Photoiniferter-Mediated Polymerization. *ACS Macro Lett.* **2020**, *9*, 613−618.
(21) Olson, R. A.; Lott, M. E.; Garrison, J. B.; Davidson, C. L. G.; Trachsel, L.; Pedro, D. I.; Sawyer, W. G.; Sumerlin, B. S. Inverse Miniemulsion Photoiniferter Polymerization for the Synthesis of Ultra-High Molecular Weight Polymers. *Macromolecules* **2022**, *55*, 8451−8460.
(22) An, Z. 100th Anniversary of Macromolecular Science Viewpoint: Achieving Ultrahigh Molecular Weights with Reversible Deactivation Radical Polymerization. *ACS Macro Lett.* **2020**, *9*, 350−357.
(23) Carmean, R. N.; Becker, T. E.; Sims, M. B.; Sumerlin, B. S. Ultra-High Molecular Weights via Aqueous Reversible-Deactivation Radical Polymerization. *Chem.* **2017**, *2*, 93−101.
(24) Wang, J.; Rivero, M.; Muñoz Bonilla, A.; Sanchez-Marcos, J.; Xue, W.; Chen, G.; Zhang, W.; Zhu, X. Natural RAFT Polymerization: Recyclable-Catalyst-Aided, Opened-to-Air, and Sunlight-Photolyzed RAFT Polymerizations. *ACS Macro Lett.* **2016**, *5*, 1278−1282.
(25) da Costa, L. P. M.; McKenzie, T. G.; Schwarz, K. N.; Fu, Q.; Qiao, G. G. Observed Photoenhancement of RAFT Polymerizations under Fume Hood Lighting. *ACS Macro Lett.* **2016**, *5*, 1287−1292.
(26) Lehnen, A. C.; Gurke, J.; Bapolisi, A. M.; Reifarth, M.; Bekir, M.; Hartlieb, M. Xanthate-Supported Photo-Iniferter (XPI)-RAFT Polymerization: Facile and Rapid Access to Complex Macromolecular Architectures. *Chem. Sci.* **2023**, DOI: 10.1039/D2SC05197D.
(27) Xia, Y.; Scheutz, G. M.; Easterling, C. P.; Zhao, J.; Sumerlin, B. S. Hybrid Block Copolymer Synthesis by Merging Photoiniferter and Organocatalytic Ring-Opening Polymerizations. *Angew. Chem. Int. Ed.* **2021**, *60*, 18537−18541.
(28) Fortenberry, A. W.; Jankoski, P. E.; Stacy, E. K.; Mccormick, C. L.; Smith, A. E.; Clemons, T. D. A Perspective on the History and Current Opportunities of Aqueous RAFT Polymerization. *Macromol. Rapid Commun.* **2022**, 2200414.
(29) Carmean, R. N.; Figg, C. A.; Scheutz, G. M.; Kubo, T.; Sumerlin, B. S. Catalyst-Free Photoinduced End-Group Removal of Thiocarbonylthio Functionality. *ACS Macro Lett.* **2017**, *6*, 185−189.
(30) Easterling, C. P.; Xia, Y.; Zhao, J.; Fanucci, G. E.; Sumerlin, B. S. Block Copolymer Sequence Inversion through Photoiniferter Polymerization. *ACS Macro Lett.* **2019**, *8*, 1461−1466.
(31) Perrier, S. 50th Anniversary Perspective: RAFT Polymerization - A User Guide. *Macromolecules* **2017**, *50*, 7433−7447.
(32) Hartlieb, M. Photo-Iniferter RAFT Polymerization. *Macromol. Rapid Commun.* **2022**, *43*, 2100514.
(33) Khan, M. Y.; Cho, M. S.; Kwark, Y. J. Dual Roles of a Xanthate as a Radical Source and Chain Transfer Agent in the Photoinitiated RAFT Polymerization of Vinyl Acetate. *Macromolecules* **2014**, *47*, 1929−1934.
(34) Li, J.; Ding, C.; Zhang, Z.; Pan, X.; Li, N.; Zhu, J.; Zhu, X. Visible Light-Induced Living Radical Polymerization of Butyl Acrylate: Photocatalyst-Free, Ultrafast, and Oxygen Tolerance. *Macromol. Rapid Commun.* **2017**, *38* (1−8), 1600482.
(35) Cabannes-Boué, B.; Yang, Q.; Lalevée, J.; Morlet-Savary, F.; Poly, J. Investigation into the Mechanism of Photo-Mediated RAFT Polymerization Involving the Reversible Photolysis of the Chain-Transfer Agent. *Polym. Chem.* **2017**, *8*, 1760−1770.
(36) Wang, H.; Li, Q.; Dai, J.; Du, F.; Zheng, H.; Bai, R. Real-Time and in Situ Investigation of "Living"/Controlled Photopolymerization in the Presence of a Trithiocarbonate. *Macromolecules* **2013**, *46*, 2576−2582.
(37) McKenzie, T. G.; da Costa, L. P. M.; Fu, Q.; Dunstan, D. E.; Qiao, G. G. Investigation into the Photolytic Stability of RAFT Agents and the Implications for Photopolymerization Reactions. *Polym. Chem.* **2016**, *7*, 4246−4253.
(38) Yeow, J.; Sugita, O. R.; Boyer, C. Visible Light-Mediated Polymerization-Induced Self-Assembly in the Absence of External Catalyst or Initiator. *ACS Macro Lett.* **2016**, *5*, 558−564.
(39) Xu, J.; Shanmugam, S.; Corrigan, N. A.; Boyer, C. Catalyst-Free Visible Light-Induced RAFT Photopolymerization. In *Controlled Radical Polymerization: Mechanisms*; Matyjaszewski, K., Sumerlin, B. S., Tsarevsky, N. V., Chiefari, J., Eds.; ACS Symposium Series; American Chemical Society: Washington, DC, 2015; pp 247−267.
(40) Young, J. B.; Bowman, J. I.; Eades, C. B.; Wong, A. J.; Sumerlin, B. S. Photoassisted Radical Depolymerization. *ACS Macro Lett.* **2022**, *11*, 1390−1395.
(41) Coyle, J. D. The Photochemistry of Thiocarbonyl Compounds. *Tetrahedron* **1985**, *41*, 5393−5425.
(42) Lehnen, A. C.; Kurki, J. A. M.; Hartlieb, M. The Difference between Photo-Iniferter and Conventional RAFT Polymerization: High Livingness Enables the Straightforward Synthesis of Multiblock Copolymers. *Polym. Chem.* **2022**, *13*, 1537−1546.
(43) McKenzie, T. G.; Fu, Q.; Wong, E. H. H.; Dunstan, D. E.; Qiao, G. G. Visible Light Mediated Controlled Radical Polymerization in the Absence of Exogenous Radical Sources or Catalysts. *Macromolecules* **2015**, *48*, 3864−3872.
(44) Thum, M. D.; Wolf, S.; Falvey, D. E. State-Dependent Photochemical and Photophysical Behavior of Dithiolate Ester and Trithiocarbonate Reversible Addition-Fragmentation Chain Transfer Polymerization Agents. *J. Phys. Chem. A* **2020**, *124*, 4211−4222.
(45) Fu, Q.; McKenzie, T. G.; Tan, S.; Nam, E.; Qiao, G. G. Tertiary Amine Catalyzed Photo-Induced Controlled Radical Polymerization of Methacrylates. *Polym. Chem.* **2015**, *6*, 5362−5368.
(46) Zhao, B.; Li, J.; Xiu, Y.; Pan, X.; Zhang, Z.; Zhu, J. Xanthate-Based Photoiniferter RAFT Polymerization toward Oxygen-Tolerant and Rapid Living 3D Printing. *Macromolecules* **2022**, *55*, 1620−1628.
(47) Moad, G.; Rizzardo, E.; Thang, S. H. Living Radical Polymerization by the RAFT Process A Second Update. *Aust. J. Chem.* **2009**, *62*, 1402−1472.

https://doi.org/10.1021/acsmacrolett.2c00683
ACS Macro Lett. 2023, 12, 14−19